REVIEW PAPER

# Application of superconducting magnetic energy storage in electrical power and energy systems: a review

Venkata Suresh Vulusala G[1,*,†] and Sreedhar Madichetty[2] (iD)

[1]EEE Department, JNTU Anantapur, Anantapur, India
[2]Birla Institute of Technology and Science, Pilani, India

## SUMMARY

Superconducting magnetic energy storage (SMES) is known to be an excellent high-efficient energy storage device. This article is focussed on various potential applications of the SMES technology in electrical power and energy systems. SMES device founds various applications, such as in microgrids, plug-in hybrid electrical vehicles, renewable energy sources that include wind energy and photovoltaic systems, low-voltage direct current power system, medium-voltage direct current and alternating current power systems, fuel cell technologies and battery energy storage systems. An extensive bibliography is presented on these applications of SMES. Also, some conclusive remarks in terms of future perspective are presented. Also, the present ongoing developments and constructions are also discussed. This study provides a basic guideline to investigate further technological development and new applications of SMES, and thus benefits the readers, researchers, engineers and academicians who deal with the research works in the area of SMES. Copyright © 2017 John Wiley & Sons, Ltd.

### Correspondence

*Venkata Suresh Vulusala G, EEE Department, JNTU Anantapur, Anantapur, India.
†E-mail: srts.venkat@gmail.com

## 1. INTRODUCTION

There are wide varieties of storage systems, for instance, compressed air energy storage, electrochemical battery energy storage systems (BESSs), pumped storage hydroelectric systems, hydrogen storage, flywheel energy storage, thermal energy storage, supercapacitors, cryogenic energy storage, liquid metal batteries, pumped thermal electricity storage and superconducting magnetic energy storage (SMES) systems. Each storage system is associated with pros and cons. BESS is considered very less because of its voltage and current limitations. Further, the chemicals were used in the manufacturing of batteries, which adversely affect the environment. Also, pumped storage hydroelectric systems depend up on its geographical locations. Hence, it may not be suitable for applications that used in day-to-day life. By overcoming all these limitations, SMES has a capability to store electric energy. The versatile and potential applications of SMES can be found in electrical energy and power systems.

The principle of operation of an SMES is when a direct current (DC) voltage is applied across the terminals of a coil, energy will be stored. The current in the coil will continue to flow even after voltage source has been removed. This is because when a superconductor is cooled less than its critical temperature, the coil attains a very less resistance that is negligible, due to which energy will be stored by generated magnetic field due to its inherent current. The energy can be discharged by its discharging coil. SMES can transit from its full-charge state to full discharge state at high speed vice versa, due to which the efficiency of SMES are very high compared with normal coils. Generally, SMES has very quick self-discharge because of its self-cooling via cryogenic liquid.

The general components of SMES are shown in Figure 1. It mainly consists of three parts: (i) low-temperature/high-temperature superconducting coil magnet, (ii) cryogenic refrigerator and (iii) helium/nitrogen liquid.

This article is mainly focussed on the application of SMES in electrical power and energy systems. This article is composed with five sections. First section gives a brief introduction about SMES. Second section deals with various applications of SMES in microgrid (MG). Further section deals with application of SMES in electrical vehicle (EV) systems. Section 4 deals with its application on renewable energy resources, and finally, it is provided with conclusive remarks with its future perspective that is given in Section 5.
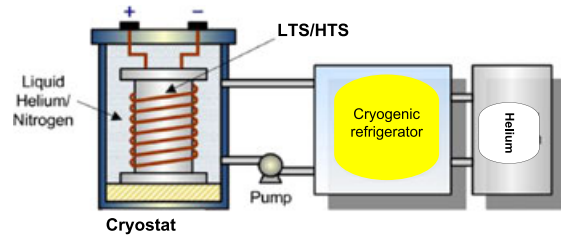
**Figure 1.** General components of superconducting magnetic energy storage. LTS, low-temperature superconductor; HTS, high-temperature superconductor. [Colour figure can be viewed at wileyonlinelibrary.com]

# 2. APPLICATION OF SUPERCONDUCTING MAGNETIC ENERGY STORAGE IN MICROGRID

## 2.1. Superconducting magnetic energy storage coil

The SMES consists of an extremely conductive coil attached to the grid by means of a power conditioning systems [1]. This acts as a constant current source and allows energy to be stored for longer duration of time without leakage and acts as a backup to inject power in the grid in case of any disturbance. The overall performance of the SMES depends on the precise configuration of these superconductive coils. The design and selection of the coil for SMES consists of two stages [2]: coil geometry decision and optimization.

## 2.2. Coil shape and design

The selection of the coil geometry in SMES is considered on the basis of factors such as stray field and available conductor length and the strain tolerance. Depending upon these criteria, there are various types of coil geometry for SMES reported till date. The three general coil geometries used are solenoid and toroid [3]. Here, various configurations of these coils are presented for comparison. In particular, the field orientation effects on the critical current and the effects on the total energy storage are examined.

## 2.3. Solenoid geometry and optimization

In comparison with toroid geometry, the solenoid geometry of the coil is simpler, can bear more mechanical stress and requires minimum wire consumption and is most cost effective solution [4]. Irrespective of high stray fields, solenoid geometry is successful for SMES for low-temperature superconductor and for small SMES as they do not need precompression and easy to coil [5,6]. Although the conventional shape of the solenoid coil is rectangular, a coil with step-shaped cross section consists of a count of coaxial coils with different lengths. This configuration is illustrated in [7]. A thin solenoid coil of

height 'h' and radius 'R', with aspect ratio $\beta = h/2R$ has proved to be promising geometry for storage. The superconductor for this kind of geometry is given by [8,9]

$$Q_{sc} = Cs(\beta)E^{2/3}B^{-1/3}, \qquad (1)$$

where 's' refers to solenoid.

The stored energy per unit of conductor is given as

$$Ks = E/Qsc = Cs(\beta)^{-1}E^{1/3}B^{1/3}. \qquad (2)$$

The results on the stored energy for the aspect ratio 0.001 and 1.0 are given later in Table I [10].

## 2.4. Toroid geometry

Whenever the 2G high-temperature superconductor (HTS) materials are considered, toroid geometry is given preference. The toroid geometry reduces the perpendicular component of the magnetic field on the conductor, which means less stray fields and presumably lower alternating current (AC) loss hence no requirement of shielding. The toroidal coils can be arranged in two ways: first, as a continuous helical winding called helical toroids, or second, as a number of short solenoids connected in series called modular toroids [11,12]. The helical toroids can be further classified on two new methods of helical winding, that is, the force-balanced coil [11] and the stress-balanced coil [13]. The stress-balanced coil is an improved design of force-balanced coil and is designed to balance the aspect ratio of coils. These designs can counterbalance high electromagnetic forces generated because of high magnetic fields and currents in the SMES. The virial theorem can optimize the structure of a helical coil and can reduce the SMES structure mass by 75% of toroidal field coil storing similar energy. The Stress-Balanced Coil (SBC) can achieve the SMES design with a superconductor of about 17% of the ampere metres of the total toroidal field coil for the same amount of energy [12]. The modular design uses short modules of solenoid connected in series and placed symmetrically. The number of small toroids influences design consideration as well as fabrication and hence ascertain feasibility of design. There are two methods used to optimize the SMES design parameters (magnetic energy, amount of superconductor and device volume): first, an object weighting method, and second, a fuzzy logic method [14,15]. Both the methods use both stray field and critical currents as constraints. This analysis

**Table I.** Thin-walled solenoids effectiveness.

| $\beta$ | 0.02 | 0.06 | 0.2 | 0.3 | 0.6 |
|---------|------|------|-----|-----|-----|
| $K_s$ | 65 | 85 | 90 | 94 | 84 |
| $C_s$ | 924 | 760 | 742 | 720 | 977 |
| $K_t$ | 74 | 84 | 85 | 72 | 64 |
| $C_s$ | 900 | 720 | 670 | 672 | 711 |

is suitable for both multiple solenoid system and modular toroid. Figure 1 represents a modular toroid configuration. Out of helical and modular coil, the helical coil has an advantage of completely enclosed magnetic field, while the modular coil leaks magnetic field outside its structure. This problem was solved by using two new coil configurations for SMES. The first one is torroid structure consisting of D-shaped solenoids with D coil filling the gaps between the circular coils. The second configuration is an *n*-polygon group, which comprise of D-shaped cross section. Both the designed worked well in $n = 4$ polygon system as shown in Figure 3 and performed well in terms of energy storage and magnetic leakage [65]. Fundamental equations and relations between inductance and coil geometry and energy stored are given as follows [3]:

The inductance of a toroidal coil is given by

$$L = \mu_o R \left( 1 - \sqrt{1 - b^2} \right), \tag{3}$$

where $b$ is the ratio of minor radius to the major radius $R$. For a total current, $I_t$, the stored energy is

$$E = \left( \mu_o R / 2 \left( 1 - \sqrt{1 - b^2} \right) \right) I_t^2. \tag{4}$$

The maximum field is

$$Bm = \left( \mu_o I_t / 2R \left( 1 - b^2 \right) \right) \Pi. \tag{5}$$

And the quantity of the conductor required for the coil is

$$Q_{sc} = 2\Pi a I_t^2 = 2\Pi R b I_t, \tag{6}$$

which can expressed in terms of the energy and field

$$Q_{sc} = 2\Pi R b I_t^{4/3} / I_t^{1/3} \tag{7}$$

$$= \left( 16\Pi^2 b^3 / \left( \mu_O (1 - b) \left( 1 - \sqrt{1 - b^2} \right)^2 \right) \right)^{1/3} E^{2/3} B^{-1/3}$$

$$= Cp(b) E^{2/3} B^{-1/3}.$$

Solving for $K = E/Q$,

$$Kp = \left( \mu_O (1 - b) \left( 1 - \sqrt{1 - b^2} \right)^2 16\Pi^2 b^3 \right)^{1/3} E^{1/3} B^{1/3}. \tag{8}$$

The values of $E/Q_{sc}$ are given in Table II for $b$ in the range 0.05 to 0.8.

Microgrid sources such as wind energy system, solar photovoltaic (PV) systems, fuel cell (FC) sources and diesel generators have been anticipated as vital components for serving rural area even without grid connection. The figure explaining the MG is shown in Figure 2. However, the important problem associated with these sources is intermittent power outputs, which may cause instability in power system. To overcome, the power fluctuations, the SMES may be better alternative that can diminish the stability problems. However, there are some concerns about the reliability problems for SMES [16]. In [16], these concerns were addressed. The reliability of SMES was addressed by a fuzzy logic-based current control strategy. The Current in SMES will be obtained by finding the energy in the circuit. Further, the same type of fuzzy logic controller in conjunction with SMES for grid-connected wind energy system was put forward. Perhaps, the dynamic performance of the grid-connected wind energy systems was not properly demonstrated in [17]. To overcome this, in [18], a hysteresis controlling scheme combined with fuzzy logic was introduced. The basic controlling scheme is shown in Figure 2. In this scheme, the magnetic field will be generated because of current passing through the coil, due to which energy will be stored in the superconducting coil. The energy from SMES will be exchanged through the DC–DC converter and DC–AC inverter. In this scheme, SMES is used in conjunction with voltage source converter to have better self-commutating capability. The DC–DC converter switching is decided by fuzzy logic control scheme, and its current and voltage control was given by hysteresis controller [18]. With this approach, small and large disturbances at grid side are drastically reduced.

Introduction of SMES in MG system enhances the voltage and power quality [19]. DC–DC converter is a static power electronic circuit, which is used to convert the DC voltage from one level to other.

Mainly, there are five versions of DC–DC converters such as, buck (step-down), boost (step-up), buck–boost (step-down/up), Cuk (step-up/down) and Sepic (step-down/up) converters. Various control mechanisms such as hysteresis controllers, pulse-width-modulated controllers, fuzzy logic-based controllers, adaptive controller, artificial neural network-based controllers and sliding mode control schemes have been applied to DC–DC converter to achieve its best voltage regulation in

**Table II.** THD comparison with and without SMES.

| Type | THD at source | | THD at load | |
| --- | --- | --- | --- | --- |
| | Voltage (%) | Current (%) | Voltage (%) | Current (%) |
| Without SMES | 8.36 | 9.32 | 11.35 | 13.52 |
| With SMES | 1.26 | 1.01 | 0.96 | 0.99 |
| Without SMES at fault | 24.32 | 26.75 | 33.42 | 38.25 |
| With SMES at fault | 8.45 | 8.65 | 16.32 | 17.21 |

THD, total harmonic distortion; SMES, superconducting magnetic energy storage.
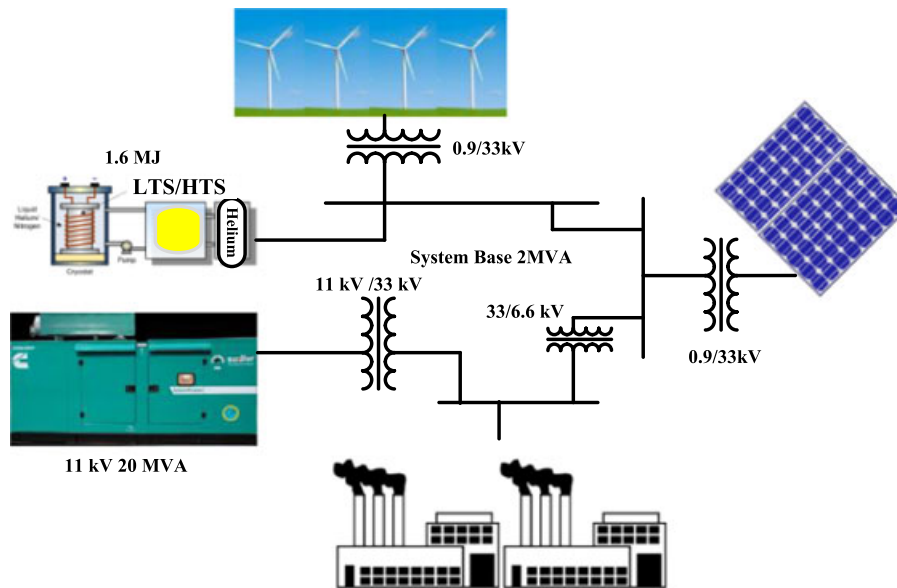
**Figure 2.** Structure of microgrid. LTS, low-temperature superconductor; HTS, high-temperature superconductor. [Colour figure can be viewed at wileyonlinelibrary.com]

conjunction with SMES. One important such implementation strategy is shown in Figure 3.

The important application of SMES in MG is to enhance its frequency regulation, power delivery and power quality in its voltage and current waveforms. The basic MG system with 1.6 MJ SME is connected with 3-MVA wind farm connected to a bus bar via 0.9/33-kV three-phase step-up transformer, which is then interconnected to PV system through a transformer of 0.9/33 kV. Also, a diesel generator of 20 MVA with its voltage rating of 11 kV is stepped up to 33 kV is connected to factory loads and is shown in Figure 1. The complete MG system has been implemented in MATLAB/Simulation with its hysteresis controlling scheme, and results have been enumerated later.

The MG system with and without SMES has been executed, and results are depicted in Figure 4. The system is subjected to 10% sudden change in factory load, which affects the DC link voltage and is shown in Figure 4(a). The DC link voltage decreased from 26 to 25 kV, which subsequently affect the load current shown in Figure 4 (b), and its results are shown in Figure 4(c) and (d), respectively. Whereas system with SMES shows DC voltage to be constant maintained at 26 kV, and its AC currents are constant without any distortion. SMES finds many applications in wind energy systems, particularly in its stability point of view [17]. The SMES is applied to DC–DC converter at the load side as well as at the terminal of wind generator. The functioning of SMES is verified with two control schemes, namely, sinusoidal pulse-width modulation scheme obtained by fuzzy logic controller and pitch control scheme. A new hysteresis control scheme has been implemented in conjunction with fuzzy control and is given in [18]. More of these kinds of SMES

application found to double fed induction generators instead of fixed speed wind generators due to its superior advantages [20]. Even in excitation systems of double-fed induction generators, SMES has been extensively used [21]. During power outages, SMES plays a vital to maintain the reactive power of connected systems, which is quite often in wind–PV-connected MG system [22]. Also, in certain cases, voltage sag and voltage swell conditions are also efficiently handled by the SMES system [23]. A further in implementation of MG system is injection of FC system. With the introduction in to PV–wind-based system, due to its intermittent nature, a new control scheme with SMES have been applied and verified [13,24].

## 3. APPLICATION OF SUPERCONDUCTING MAGNETIC ENERGY STORAGE IN ELECTRICAL VEHICLE AND RENEWABLE ENERGY SYSTEM

Electrical vehicles projected to be future for personal and commercial transportation, which then increases load requirement in MG that is uncertain. The abrupt power charging of EV results in load fluctuations that subsequently introduce harmonics into the system. Many researches are focussed on the suitable control schemes for abrupt power charging when it connected to MG. Problem becomes more severe in MG due to intermittent power by PV and wind systems. Hence, there is a necessity to fill the gap between intermittent power by renewable sources and EV. Various superconducting energy schemes have been discussed in [25].
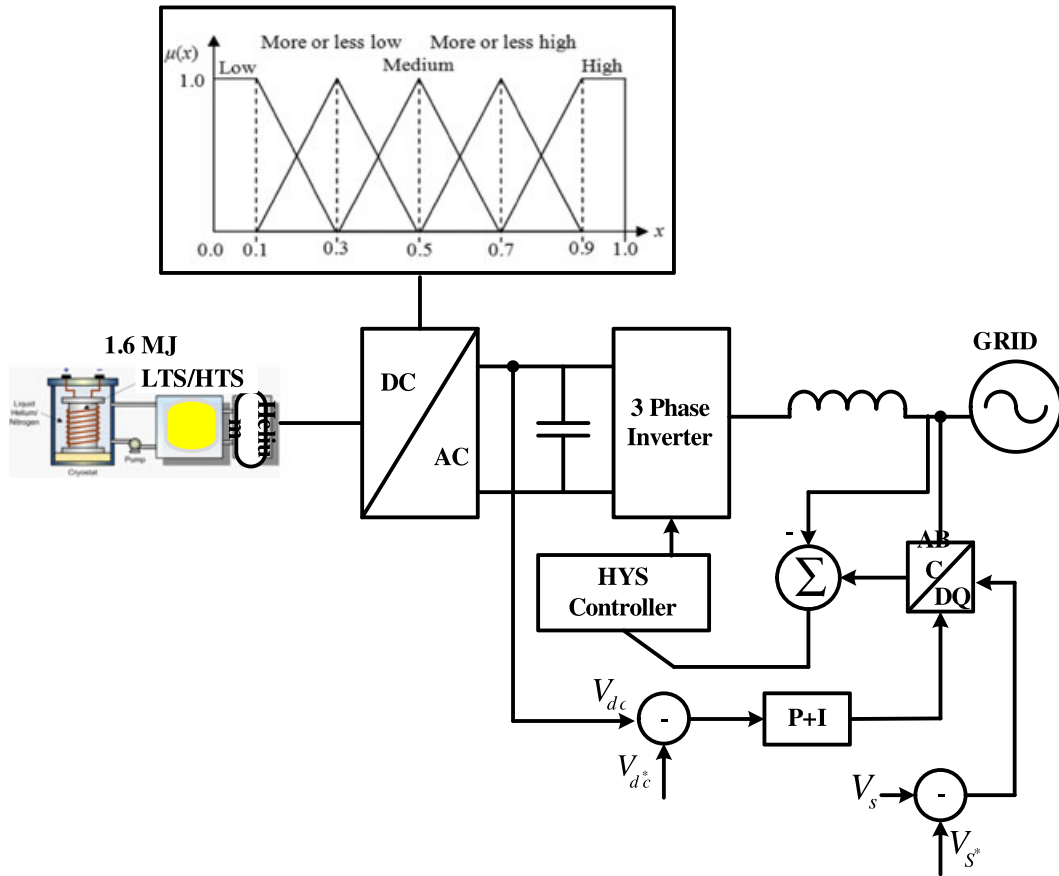
**Figure 3.** Hysteresis (HYS) and fuzzy logic-based control scheme. LTS, low-temperature superconductor; HTS, high-temperature superconductor; AC, alternating current; DC, direct current; HYS, hysteresis. [Colour figure can be viewed at wileyonlinelibrary.com]
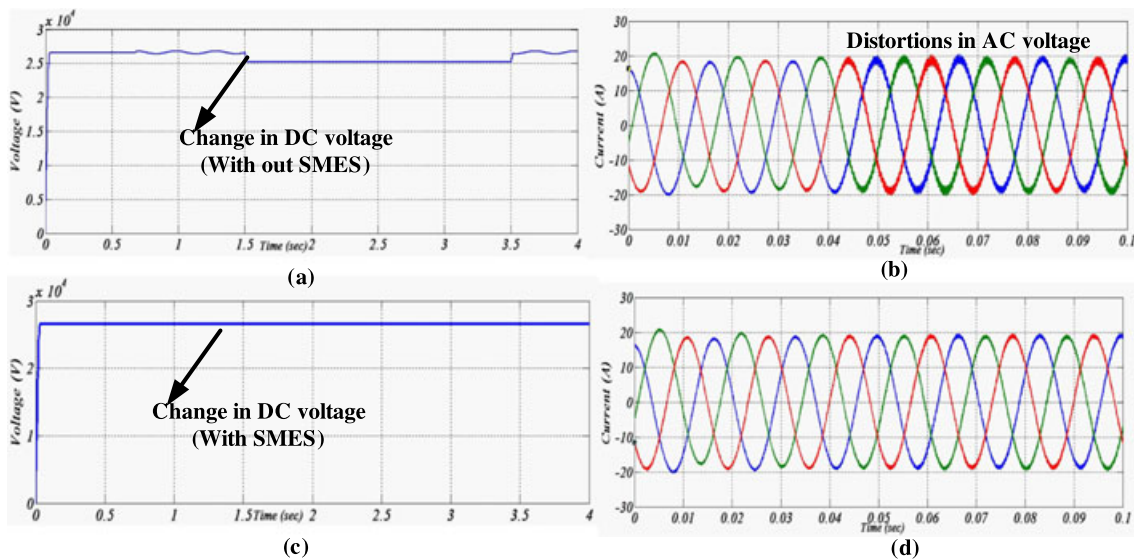


**Figure 4.** Effect of superconducting magnetic energy storage (SMES) in microgrid system in direct current (DC) link voltage and alternating current (AC) side currents. [Colour figure can be viewed at wileyonlinelibrary.com]

Electrical vehicle-connected MG system is shown in Figure 5(a). The charging station is operated with 400 V. However, the system controllers mainly depend up on the DC–DC converter and DC–AC converter. The individual converter scheme is shown in Figure 5(b). Each inverter is controlled by its voltage and current controller. The output of the inverter is then connected to filter, which subsequently reduces the harmonics in the system. To analyse the stability of system, a small signal model has to be developed.

### 3.1. Small signal model of diesel generator

The diesel generator consists of a diesel engine, valve actuator and speed control loop. Input to the model is load $P_L$, that is, output power of the electrical generator. The transfer function of valve actuator, diesel engine and rotor swing equations could be written as follows:

$$\frac{\Delta X_1(s)}{\Delta X_2(s)} = \frac{1}{1 + ST_{sm}} \qquad (9)$$
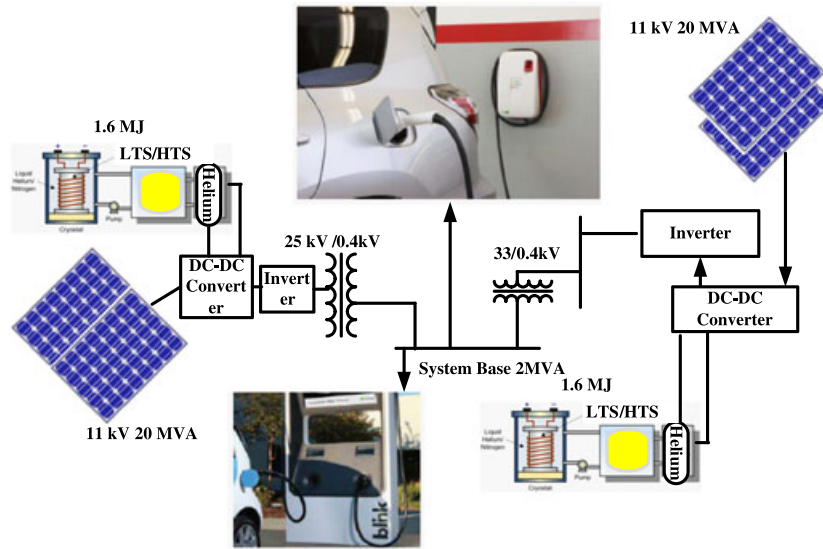


(a) . Micro Grid system connected Electrical Vehicle system
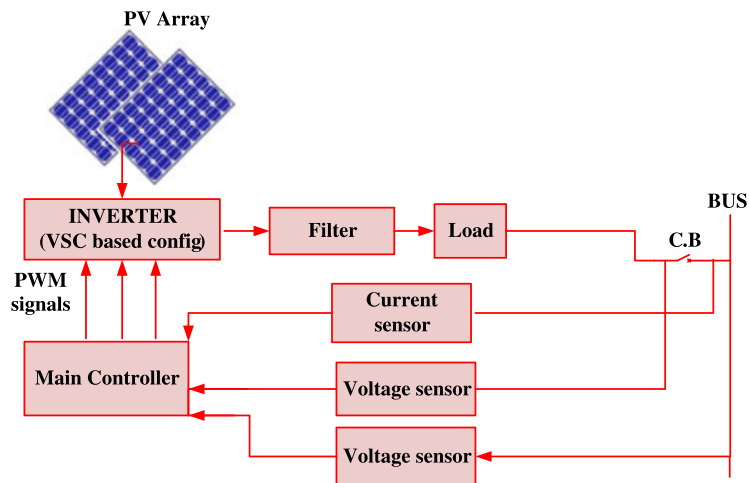


(b) . Micro Grid system connected Electrical Vehicle system

**Figure 5.** (a) Microgrid system-connected electrical vehicle system and (b) microgrid system-connected electrical vehicle system. LTS, low-temperature superconductor; HTS, high-temperature superconductor; DC, direct current; PV, photovoltaic; PWM, pulse-width modulation; VSC, voltage source converter. [Colour figure can be viewed at wileyonlinelibrary.com]

$$\frac{\Delta X_2(s)}{\Delta X_3(s)} = \frac{1}{1 + ST_d}. \qquad (10)$$

The complete transfer function model is given in Figure 6(a).

## 3.2. Transfer function model of fuel cell

The dynamic model of FC system depends up on the injection of stored energy. For small signal studies, the FC can be modelled with fuel blocks, an inverter and an interconnection. The time constant of fuel block, inverter and an interconnecting device could be taken as $T_{fc}$, $T_1$ and $T_2$, respectively. The complete transfer

function is given in Eqn (11), and its block diagram is shown in Figure 6(b).
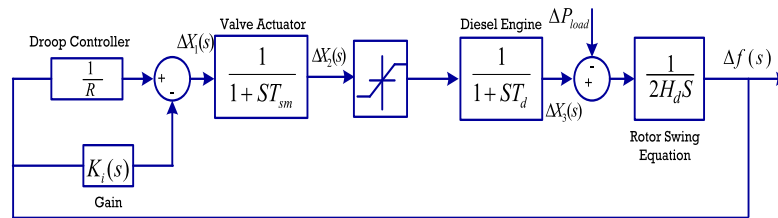
$$F(s) = \frac{1}{(1 + ST_1)(1 + ST_2)(1 + ST_{fc})}. \qquad (11)$$

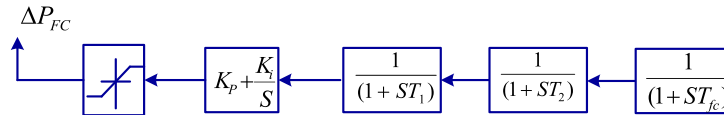## 3.3. Transfer function model of photovoltaic generating systems

The output power in PV system can be given as

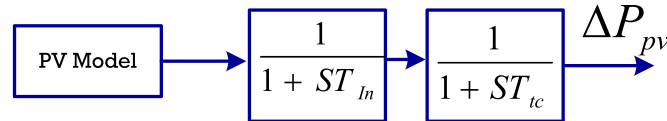$$P_{pv} = \eta s \phi \{1 - 0.005(T_a + 25)\}. \qquad (12)$$

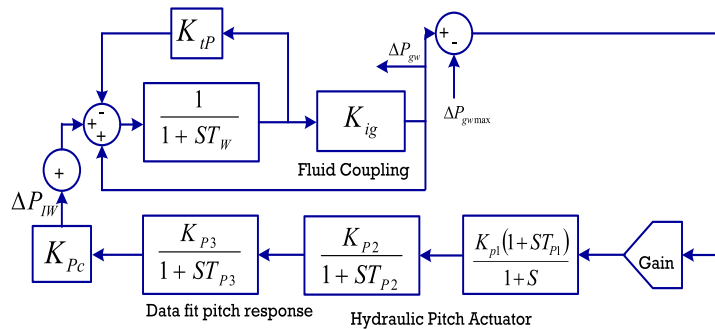The transfer function for PV cell can be written as



(a) Transfer function model of diesel energy generator

(b) Transfer function model of fuel cell system

(c) Transfer function model of PV system

(d) Transfer function model of wind energy system system

**Figure 6.** (a) Transfer function model of diesel energy generator, (b) transfer function model of fuel cell system, (c) transfer function model of photovoltaic (PV) system and (d) transfer function model of wind energy system. [Colour figure can be viewed at wileyonlinelibrary.com]

$$\frac{K_{PV}}{1 + ST_{PV}}, \qquad (13)$$

and its complete block diagram is shown in Figure 6(c).

## 3.4. Transfer function model of wind energy generating systems

The total power captured by the wind turbine is given as

$$P_w = \frac{1}{2} * \rho * A * V^3$$

$\rho = 1.225$ kg/m$^3$ (sea level, 15$^o$); $A = \pi * R^2$ (total area of the turbine blades).

$C_P$ is extracted as a function of $\lambda$ that is 'tip speed ratio'; similarly, $\beta$ is pitch angle expression that is given as
$\lambda = (\omega * R)/V$.

The developed relation between $C_P$ and $\lambda$ is normally recognized by the $C_P/\lambda$ curve. This curve mostly gives the efficiency of the turbine; its most important developing turbine expression is given as

$$\frac{1}{\lambda_i} = \frac{1}{\lambda + 0.08*\beta} - \frac{0.035}{\beta^3 + 1}$$

where the coefficients of constants are $C_1 = 0.5176$, $C_2 = 116$, $C_3 = 0.4$, $C_4 = 5$, $C_5 = 21$ and $C_6 = 0.0068$. The complete block diagram of wind energy system is
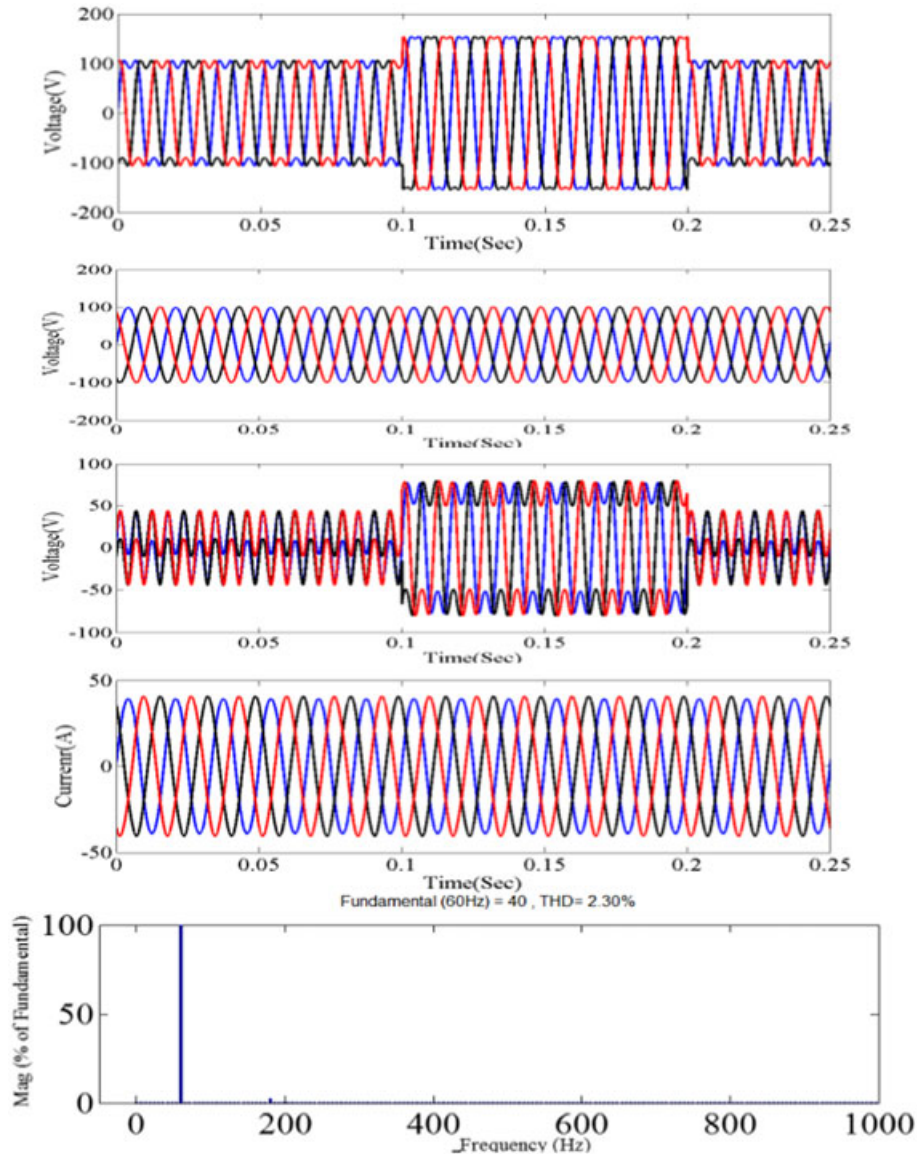


**Figure 7.** (From top to bottom) (a) Voltage subjected to sag, (b) voltage at the terminals of charging station, (c) voltage subjected to swell conditions, (d) current at the charging station and (e) total harmonic distortion waveform of voltage. [Colour figure can be viewed at wileyonlinelibrary.com]

given in Figure 6(d). The entire system has been integrated as shown in Figure 4(a) and tested MATLAB/Simulation environment, and its results are listed in Figure 7. The complete system nomenclature can be found in [13].

Various controller gains, for instance, proportional controller, integral controller and derivative controller, have been chosen at an optimum level with an objective to achieve best in performance at its voltage and current wave form and subsequently to minimize the total harmonic distortion. The system has been subjected to various sag and swell conditions with simultaneous abrupt charging of EV. MG system has been prone sag condition from 0.1 to 0.2 s and swell condition from 0.1 to 0.2 s.

In the both cases, the output voltage and output current found constant and which were due to SMES. Finally, the total harmonic distortion of output voltage has also been tested and found with exciting 2.30% with all lower order harmonics eliminated. All these results are shown in Figure 7.

The proposed system has been executed with and without SMES, and its results have been tabulated in Table II. From which, it is clear that system with SMES is able to reduce the harmonic content and able perform better with SMES.

Superconducting magnetic energy storage has good control over the load conditions as well, and it is shown in Figure 8. As per load demand, the SMES participated in actively and able to maintain the load voltage as constant. Further, with the ability of control in voltage, it leads to

less circulating currents. Mitigation of circulating currents leads to improvement of power transfer capability.

# 4. OTHER APPLICATIONS AND FUTURE PROSPECTUS OF SUPERCONDUCTING MAGNETIC ENERGY STORAGE

The basic design of 10-kJ class SMES can be found in [26], high-filed HTS SMES coil [27], 200-kJ 2G HTS solenoidal SMES coil can be found in [28], and their thermal and cooling design can be found in [29]. The SMES founds application in mitigating the wind energy system fluctuations [30], voltage harmonics [31] and enhancing stability [32], and its modern prospectus applications are given in [33,34]. Robust controller schemes such as fuzzy logic, hysteresis, H-infinity and sliding mode control schemes have been applied to SMES in conjunction with voltage source converter in MG [32,35,36]. High power superconduction power station have been started and function at China [37]. Several power control schemes in conjunction with the SMES have been developed for frequency regulation, reactive power control, speed control and power charging [31,36,38–41]. In near future, SMES can acquire a very prominent place in EV system, space shuttles, satellites system and even in medical applications as well.
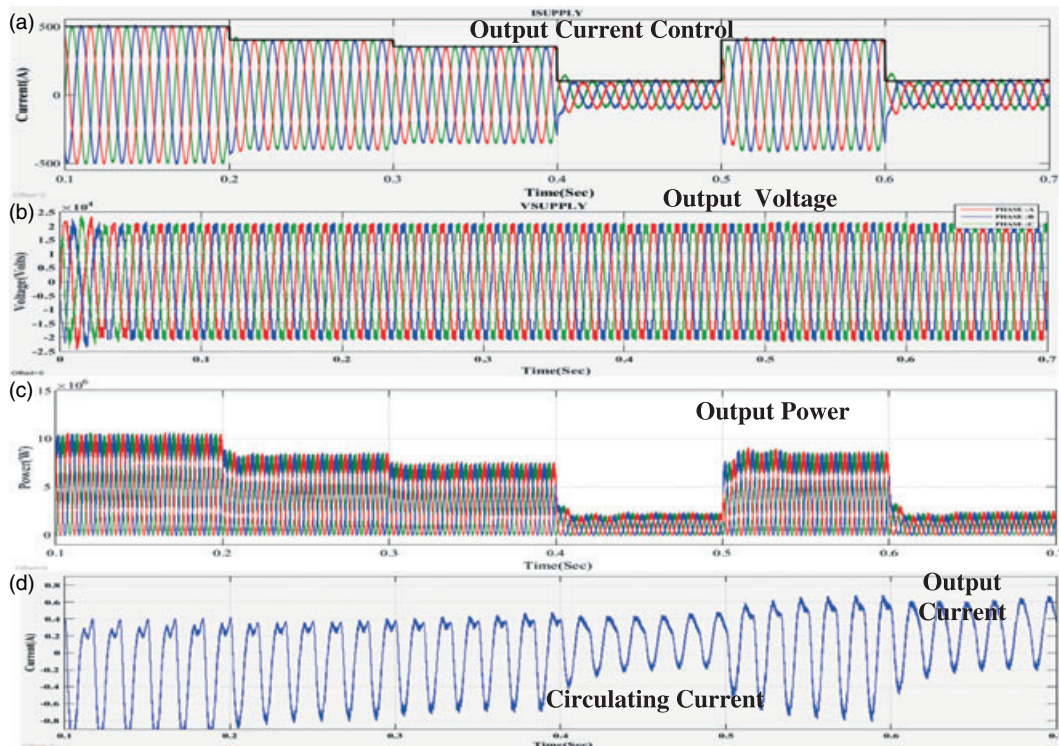


**Figure 8.** (From top to bottom) (a) Current subjected to various loading conditions, (b) voltage at the load terminals, (c) output power varying conditions and (d) revolving current reduction. [Colour figure can be viewed at wileyonlinelibrary.com]

## 5. CONCLUSION

In this article, various potential applications of the SMES technology in electrical power and energy systems have been discussed. Mainly, SMES applications, such as in MGs, plug-in hybrid EVs, renewable energy sources, which includes wind energy and PV systems, low-voltage direct current power system, medium-voltage direct current and alternating current power systems, FC technologies and BESSs, have been extensively discussed.

## REFERENCES

1. Morandi A. Design and comparison of a 1-MW/5-s HTS SMES with toroidal and solenoidal geometry. *IEEE Transactions on Applied Superconductivity* 2016; **26**(4).

2. Kim JH, Hahn S-y. Design of a 200-kJ HTS SMES system. *IEEE Transactions on Applied Superconductivity* 2002; **12**(1).

3. Hassenzahl W. A comparison of the conductor requirements for energy storage devices made with ideal coil geometries. *IEEE Transactions on Magnetics* 1989; **25**(2).

4. Schoenung SM, Meier WR, Hassenzahl WV. A comparison of large-scale toroidal and solenoidal SMES systems. *IEEE Transactions on Magnetics* 1991; **27**(2):2324–2328.

5. Boenig HJ, Hauer JF. Commissioning tests of the Bonneville power administration 30 MJ superconducting magnetic energy storage unit. *IEEE Trans. Power Appl. Syst.* 1985; **PAS-104**(2):302–312.

6. Nagaya S *et al.* The state of the art of the development of SMES for bridging instantaneous voltage dips in Japan. *Cryogenics* 2012; **52**(12):708–712.

7. Noguchi S, Yamashita M, Yamashita H, Ishiyama A. An optimal design method for superconducting magnets using HTS tape. *ieee transactions on applied superconductivity* 2001; **11**(1):2308.

8. Nomura S, Ajiki D, Suzuki C, Watanabe N, Koizumi E, Tsutsui H, Tsuji-Iio S, Shimada R. Design considerations for force-balanced coil applied to SMES. *IEEE Transactions on Applied Superconductivity* 2001; **11**(1):1920.

9. Nomura S, Yamagata K, Ajiki D, Watanabe N, Ajikawa H, Tsuji-Iio S, Shimada R, Kyouto M, Sato Y. Experiment of HTS stress-balanced helical coil. *IEEE Trans. Applied. Supercond.* 2000; **10**(1):820.

10. Miura Y, Sakota M, Shimada R. Force-free coil principle applied to helical winding. *IEEE Transactions on Magnetics* 1994; **30**(4) p 2573 5.

11. Sato Y., Kondoh J., Shimada R., Kyouto M., Hanai S. and Hamajima T., "Experiment of the force-balanced coil for superconducting magnetic energy storage." Proceedings of the 15th International Conference on Magnet Technology (MT-15),(1997) p 542.

12. Borghi CA, Fabbri M, Ribani PL. Design optimisation of a microsuperconducting magnetic energy storage system. *IEEE Trans. Magnetics* 1999; **35**(5) p4275 7.

13. Liu Y, Tang Y, Shi J, Shi X, Deng J, Gong K. Application of small-sized SMES in an EV charging station with DC bus and PV system," in. *IEEE Transactions on Applied Superconductivity* 2015; **25**(3):1–6. https://doi.org/10.1109/TASC.2014.2374174.

14. Birkner PJ. On the design of superconducting magnetic energy storage systems. *IEEE Transactions on Applied Superconductivity* 1993; **3**(1):p246.

15. Vincent-Viry O, Mailfert A, Trassart D. New SMES structures analysis. *IEEE Transactions on Applied Superconductivity* 2001; **11**(1):1916.

16. Gong K, Shi J, Liu Y, Wang Z, Ren L, Zhang Y. Application of SMES in the microgrid based on fuzzy control," in. *IEEE Transactions on Applied Superconductivity* 2016; **26**(3):1–5. https://doi.org/10.1109/TASC.2016.2524446.

17. Ali MH, Park M, Yu IK, Murata T, Tamura J. Improvement of wind-generator stability by fuzzy-logic-controlled SMES," in. *IEEE Transactions on Industry Applications* 2009; **45**(3):1045–1051. https://doi.org/10.1109/TIA.2009.2018901.

18. Yunus MS, Abu-Siada A, Masoum MAS. Improving dynamic performance of wind energy conversion systems using fuzzy-based hysteresis current-controlled superconducting magnetic energy storage," in. *IET Power Electronics* 2012; **5**(8):1305–1314. https://doi.org/10.1049/iet-pel.2012.0135.

19. Kreeumporn W, Ngamroo I. Optimal superconducting coil integrated into PV generators for smoothing power and regulating voltage in distribution system with PHEVs," in. *IEEE Transactions on Applied Superconductivity* 2016; **26**(7):1–5. https://doi.org/10.1109/TASC.2016.2591981.

20. Shiddiq Yunus M, Abu-Siada A, Masoum MAS. Application of SMES unit to improve DFIG power dispatch and dynamic performance during intermittent misfire and fire-through faults," in. *IEEE Transactions on Applied Superconductivity* 2013; **23**(4, pp. 5701712-5701712). https://doi.org/10.1109/TASC.2013.2256352.

21. Shi J, Tang Y, Xia Y, Ren L, Li J. SMES based excitation system for doubly-fed induction generator in wind power application," in. *IEEE Transactions on Applied Superconductivity* 2011; **21**(3):1105–1108. https://doi.org/10.1109/TASC.2011.2105450.

22. Kim ST, Kang BK, Bae SH, Park JW. Application of SMES and grid code compliance to wind/photovoltaic generation system," in. *IEEE*

*Transactions on Applied Superconductivity* 2013; **23**(3, pp. 5000804-5000804). https://doi.org/10.1109/TASC.2012.2232962.

23. Yunus MS, Masoum MAS, Abu-Siada A. Application of SMES to enhance the dynamic performance of DFIG during voltage sag and swell," in. *IEEE Transactions on Applied Superconductivity* 2012; **22**(4, pp. 5702009-5702009). https://doi.org/10.1109/TASC.2012.2191769.

24. Hamajima T *et al.* Application of SMES and fuel cell system combined with liquid hydrogen vehicle station to renewable energy control," in. *IEEE Transactions on Applied Superconductivity* 2012; **22**(3, pp. 5701704-5701704). https://doi.org/10.1109/TASC.2011.2175687.

25. Morandi L, Trevisani F, Negrini P, Ribani L, Fabbri M. Feasibility of superconducting magnetic energy storage on board of ground vehicles with present state-of-the-art superconductors," in. *IEEE Transactions on Applied Superconductivity* 2012; **22**(2, pp. 5700106-5700106). https://doi.org/10.1109/TASC.2011.2177266.

26. Kim AR *et al.* Design of a 10 kJ class SMES model coil for real time digital simulator based grid connection study," in. *IEEE Transactions on Applied Superconductivity* 2009; **19**(3):2023–2027. https://doi.org/10.1109/TASC.2009.2018494.

27. Gupta R *et al.* Design, construction, and testing of a large-aperture high-field HTS SMES coil," in. *IEEE Transactions on Applied Superconductivity* 2016; **26**(4):1–8. https://doi.org/10.1109/TASC.2016.2517404.

28. Trillaud F, Cruz LS. Conceptual design of a 200-kJ 2G-HTS solenoidal μ-SMES," in. *IEEE Transactions on Applied Superconductivity* 2014; **24**(3):1–5. https://doi.org/10.1109/TASC.2013.2284478.

29. Jiao F *et al.* Electromagnetic and thermal design of a conduction-cooling 150 kJ/100 kW hybrid SMES system," in. *IEEE Transactions on Applied Superconductivity* 2013; **23**(3, pp. 5701404-5701404). https://doi.org/10.1109/TASC.2012.2234926.

30. Lee J, Kim JH, Joo SK. Stochastic method for the operation of a power system with wind generators and superconducting magnetic energy storages (SMESs)," in. *IEEE Transactions on Applied Superconductivity* 2011; **21**(3):2144–2148. https://doi.org/10.1109/TASC.2010.2096491.

31. Abu-Siada, Islam S. Application of SMES unit in improving the performance of an AC/DC power system," in. *IEEE Transactions on Sustainable Energy* 2011; **2**(2):109–121. https://doi.org/10.1109/TSTE.2010.2089995.

32. Dechanupaprittha S, Sakamoto N, Hongesombut K, Watanabe M, Mitani Y, Ngamroo I. Design and analysis of robust SMES controller for stability enhancement of interconnected power system taking coil size into consideration," in. *IEEE Transactions on Applied Superconductivity* 2009; **19**(3):2019–2022. https://doi.org/10.1109/TASC.2009.2018492.

33. Wan Y, Zhao J. $H_\infty$ control of single-machine infinite bus power systems with superconducting magnetic energy storage based on energy-shaping and backstepping," in. *IET Control Theory & Applications* 2013; **7**(5):757–764. https://doi.org/10.1049/iet-cta.2012.0897.

34. Chen XY *et al.* Integrated SMES technology for modern power system and future smart grid," in. *IEEE Transactions on Applied Superconductivity* 2014; **24**(5):1–5. https://doi.org/10.1109/TASC.2014.2346502.

35. Molina MG, Enrique Mercado P, Hirokazu Watanabe E. Improved superconducting magnetic energy storage (SMES) controller for high-power utility applications," in. *IEEE Transactions on Energy Conversion* 2011; **26**(2):444–456. https://doi.org/10.1109/TEC.2010.2093601.

36. Ali MH, Wu B, Dougal RA. An overview of SMES applications in power and energy systems," in. *IEEE Transactions on Sustainable Energy* 2010; **1**(1):38–47. https://doi.org/10.1109/TSTE.2010.2044901.

37. Zhang G *et al.* The construction progress of a high-Tc superconducting power substation in China," in. *IEEE Transactions on Applied Superconductivity* 2011; **21**(3):2824–2827. https://doi.org/10.1109/TASC.2010.2098471.

38. Chen Z, Xiao XY, Li CS, Zhang Y, Zheng ZX. Study on unit commitment problem considering large-scale superconducting magnetic energy storage systems," in. *IEEE Transactions on Applied Superconductivity* 2016; **26**(7):1–6. https://doi.org/10.1109/TASC.2016.2598353.

39. Zhang JY *et al.* Electric energy exchange and applications of superconducting magnet in an SMES device," in. *IEEE Transactions on Applied Superconductivity* 2014; **24**(3):1–4. https://doi.org/10.1109/TASC.2013.2291438.

40. Xiao L, Lin L. Recent progress of power application of superconductor in China," in. *IEEE Transactions on Applied Superconductivity* 2007; **17**(2):2355–2360. https://doi.org/10.1109/TASC.2007.898160.

41. Jin JX, Chen XY. Cooperative operation of superconducting fault-current-limiting cable and SMES system for grounding fault protection in a LVDC network," in. *IEEE Transactions on Industry Applications* 2015; **51**(6):5410–5414. https://doi.org/10.1109/TIA.2015.2438252.